Title

Epistatic Transcription Factor Networks Differentially Modulate Arabidopsis Growth and Defense

Baohua Li[1*], Michelle Tang[1,2*], Céline Caseys[1*], Ayla Nelson[1], Marium Zhou[1], Xue Zhou[1], Siobhan M. Brady[2], and Daniel J. Kliebenstein[1,3 x]

[1]Department of Plant Sciences, University of California, Davis, One Shields Avenue, Davis, CA, 95616, USA

[2]Department of Plant Biology and Genome Center, University of California, Davis, One Shields Avenue, Davis, CA, 95616, USA

[3]DynaMo Center of Excellence, University of Copenhagen, Thorvaldsensvej 40, DK-1871, Frederiksberg C, Denmark

*These authors contribute equally to this study

[x]Corresponding Author: Kliebenstein@ucdavis.edu

The author responsible for distribution of materials is: Daniel J. Kliebenstein (Kliebenstein@ucdavis.edu).

ORCID IDs: 0000-0001-7235-0470 (B.L.); 0000-0002-8779-8697 (M.T.); 0000-0003-4187-9018 (C.C.); 0000-0002-2586-0264 (X.Z.); 0000-0001-9424-8055 (S.M.B.); 0000-0001-5759-3175 (D.J.K.)

Abstract

Plants integrate internal and external signals to finely coordinate growth and defense allowing for maximal fitness within a complex environment. One common model for the relationship between growth and defense is a trade-off model in which there is a simple negative interaction between growth and defense theoretically driven by energy costs. However, there is a developing consensus that the coordination of growth and defense likely involves a more conditional and intricate connection. To explore how a transcription factor network may coordinate growth and defense, we used high-throughput phenotyping to measure growth and flowering in a set of single and pairwise mutants previously linked to the aliphatic glucosinolate defense pathway. Showing the link between growth and aliphatic glucosinolate defense, 17 of the 20 tested TFs significantly influence plant growth and/or flowering time. These effects were conditional upon the environment, age of the plant and more critically varied amongst the phenotypes when using the same genotype. The phenotypic effects of the TF mutants on SC GLS accumulation and on growth did not display a simple correlation, supporting the coordination model. We propose that large transcription factor networks create a system to integrate internal and external signals and separately modulate growth and the accumulation of the defensive aliphatic GLS.

Introduction

Growth and defense are essential biological processes necessary for plant survival. Optimizing fitness requires plants to coordinate growth and defense phenotypes in response to specific environments. Efforts to understand the relationship between plant growth and defense is often modeled as a trade-off where resistance is a cost on growth (KARBAN and BALDWIN 1997; AGRAWAL 2011a; AGRAWAL 2011b; HUOT *et al.* 2014). This model assumes that the available resources for plants are limited, suggesting that any flux of resources, energy and elements into plant defense would be at the cost of lost plant growth. Support for this model comes from the observations that some constitutive defense mutants generally grow smaller and suffer from yield and/or fitness losses.

A developing model is emerging from research in ecology, evolutional biology and molecular genetics that suggests a dynamic relationship between plant defense and growth (SINGH *et al.* 2002; DE LUCAS *et al.* 2016). Multiple reports showed that defense metabolism does not show a universal negative correlation with plant growth (BERGELSON and PURRINGTON 1996; ALMEIDA-CORTEZ *et al.* 1999; KORICHEVA 2002). Mechanistic manipulations of defense metabolism have also shown little to no effect on plant growth. Further, diminutive constitutive defense mutants can have their growth rescued by second site mutations that maintain the constitutive defense (HEMM *et al.* 2003; PAUL-VICTOR *et al.* 2010; ZÜST *et al.* 2011; JOSEPH *et al.* 2013; CAMPOS *et al.* 2016; KLIEBENSTEIN 2016). Specific TFs are also being identified that can simultaneously increase growth and specific defenses (CAMPOS *et al.* 2016; WANG *et al.* 2018). Together, these observations suggest that the relationship between plant defense and growth is a complex and active internal decision process involving regulatory and signaling pathways *in planta* (ZUST and AGRAWAL 2017). Systemic and large scale studies are needed to fully explore the relationship between plant growth and defense, ideally in a highly characterized model system for both plant growth and defense.

Both plant growth and defense are regulated by complex signaling pathways, in which transcriptional factors (TFs) play key roles in integrating and transducing internal and external signals (SINGH *et al.* 2002; PAJEROWSKA-MUKHTAR *et al.* 2012; LOZANO-DURAN *et al.* 2013; FAN *et al.* 2014; DE LUCAS *et al.* 2016). Several recent studies provide important insights about the roles TFs played in coordinating growth and defenses. Mutations of *JAZ*s, transcriptional repressors in jasmonic acid (JA) signaling pathway, in combination with altered photoreceptor

PhyB results in fast-growing plants with enhanced plant defense responses (CAMPOS *et al.* 2016). A rice TF, *Ideal Plant Architecture 1 (IPA)*, was previously cloned and characterized to activate yield-related genes and promote the high yield (JIAO *et al.* 2010), and recently further shown to promote both plant defense and rice yield simultaneously (WANG *et al.* 2018). These case studies demonstrated that growth and defense are under complex regulation and TFs are key integrators that coordinate these two important biological processes. However, it is not clear if these are isolated instances or a more generalizable view of how TFs modulate growth and defense. Systemic studies with well selected and designed experiments on TFs and their regulatory networks are needed to test how TFs may or may not coordinate between plant defense and growth in diverse environmental settings.

To explore the interplay between plant growth and defense, we used the classical and well-studied plant secondary metabolic pathway, the Arabidopsis methionine-derived aliphatic glucosinolates (GLS) (SØNDERBY *et al.* 2010b). The aliphatic GLS have been shown to provide defense against numerous herbivorous insects in both the lab and the field (LAMBRIX *et al.* 2001; SCHLAEPPI *et al.* 2008; KOS *et al.* 2012; BERAN *et al.* 2014; FALK *et al.* 2014; KERWIN *et al.* 2015; KERWIN *et al.* 2017; ZALUCKI *et al.* 2017). Aliphatic GLS are critical for fitness in Brassicales and their specific composition and accumulation across developmental stages are intricately controlled by genetic variation and influence many important biological processes (KLIEBENSTEIN *et al.* 2002; BIDART-BOUZAT and KLIEBENSTEIN 2008; WENTZELL and KLIEBENSTEIN 2008; BUROW *et al.* 2010; KERWIN *et al.* 2011; ZÜST *et al.* 2011). Thus, the aliphatic GLS are a key defense system within the Brassicales. Flux-based modeling suggests aliphatic GLS should be expensive to produce since they contain both sulfur and nitrogen and accumulate to high levels. However, mutants missing these compounds have at most a slight change in early growth, indicating that aliphatic GLS do not display a tight trade-off with growth (PAUL-VICTOR *et al.* 2010; ZÜST *et al.* 2011; BEKAERT *et al.* 2012). Instead, the regulatory complexity of the aliphatic GLS better fits with the coordination model. For example, a large scale yeast one-hybrid study identified a large collection of TFs that regulate aliphatic GLS accumulation (LI *et al.* 2014). These TFs bind the aliphatic GLS enzyme promoters, directly arguing against a single dominant TF model. Further, these TFs showed extensive epistatic interactions in influencing the accumulation of GLS (LI *et al.* 2018). This suggests that the regulation of this defense pathway is highly complex. However, previous studies did not inform

on whether these TFs linked to aliphatic GLS have individual or epistatic effects on growth or flowering.

To test if growth and defense are linked by this epistatic network of TFs, we used a high throughput method to measure growth and flowering time of 20 single TF mutants and 48 double mutants previously shown to influence the Arabidopsis aliphatic GLS pathway in two environments (SØNDERBY *et al*. 2007; LI *et al*. 2018). We show that 17 of the 20 TFs significantly influence plant growth and/or plant flowering time. While most TFs influence growth and defense, there was no clear correlation between the aliphatic short chain (SC) GLS accumulation and plant growth and flowering time in our study. This indicates that each TF has specific and independent influences on both growth and aliphatic GLS. Our findings support the coordination model for the relationship between plant growth and aliphatic GLS, and provide novel insights on how these critical and complex biological processes are integrated to optimize fitness in different environments.

Results

Conditional Growth Effects of the 20 TF Mutations

The 20 selected TFs for this study were originally identified as binding aliphatic GLS related promoters and their knockout mutants influence aliphatic GLS accumulation (LI *et al.* 2014; LI *et al.* 2018). In this study, we focused on the aliphatic GLS as they are ~90% of the total GLS content within Arabidopsis leaves representing the majority of the metabolic flux. To measure growth variation in this mutant collection which have altered defense levels that are within the range of variation occurring within natural accessions (KLIEBENSTEIN *et al.* 2001), we utilized digital image analysis to measure plant size in two chambers, CEF clean chamber and LSA herbivore chamber (LI *et al.* 2018). Growth was measured every other day from 9 days post-germination to 27 days at which time the leaves were overlapping. Plants were organized in a randomized complete block design with 8 measurements per genotype per chamber (LI *et al.* 2018). The two growth chambers differed in the presence or absence of mites, flea beetles and fungus gnat larvae, allowing us to test how the underlying networks respond to complex environmental perturbations. To maintain this difference, CEF was cleaned monthly while LSA had long term tomato and Brassica plants that sustained the endogenous pest population. The plant growth measurement spans the majority of vegetative growth providing a dynamic analysis

of growth. Combining the data with linear models, we tested for significant effects of all single gene TF mutants on growth across the conditions (Figure 1, Supplemental Figure 1 and Supplemental Data Set 1, 2). To reduce false positives, we required a TF to have at least 2 significant hits across the days in the TF and/or treatment conditioned TF effect to be validated as TF influencing plant growth.

The influence of these TFs on growth is highly conditional on both plant age and growth chamber (Figure 1 and Supplemental Figure 2). 15 of the 20 aliphatic GLS TF mutants had a significant influence on growth. Stronger positive growth effects were observed more often in the herbivore LSA chamber than in the clean CEF chamber for a number of TFs like *HMGBD15*, *AT5G52020*, *ZFP4*, *CBF4*, *NAC102*, and *GBF2* (Figure 1). In contrast, *ABF4* had strong negative growth effects in both chambers. In addition to differences between the growth chambers, there were TFs that had differential influence across plant age. For example, *GBF2* has growth effects across most plant stages while *nac102* only shows a significant phenotype during early vegetative growth (Figure 1). Some mutants combined these conditionality's as illustrated by *ilr3*, which had a transition at 21 days post germination from positive to negative growth effects. This conditionality illustrates the importance of large-scale phenotyping across different conditions to generate a broad view of how mutational effects may change dynamically (Supplemental Figure 1 and 2). In an energetic tradeoff, we would expect that most of these TF mutations should lead to smaller plants as these mutations increase aliphatic GLS content (LI *et al*. 2014). In contrast, the mutants had a mix of positive and negative growth effects. In addition, three mutants with strong aliphatic GLS phenotypes, *ant*, *myb28* and *myb29*, have little to no detectable main effect on growth. Although an alternative explanation for the *myb28/29* mutant is that this mutation has a ~2x increase in indolic GLS accumulation and this may balance the loss in aliphatic GLS. However, because aliphatic GLS are ~90% of the total GLS, this slight increase in indolic GLS means that the *myb28/29* double mutant has a loss of 80% of total GLS flux. The links between plant growth and defense via the aliphatic GLS in this TF collection supports the coordination model of growth and defense.

Dynamic Epistatic Networks Underlying Plant Growth

We previously generated a set of 48 pairwise mutant combinations from these 20 TFs that identified an extensive antagonistic epistatic network of the 20 TFs controlling aliphatic GLS

(SØNDERBY *et al.* 2007; LI *et al.* 2018). As these TFs had affected growth individually, we used linear models to assess if the epistatic effects were as prevalent on growth as on aliphatic GLS accumulation. We plotted the significant interactions on growth for five different days on the aliphatic GLS epistatic network (Figure 2A-E, and Supplemental Data Set 3, 4). This analysis identified extensive epistatic interactions influencing growth. As observed in the single mutants, the epistatic interactions were equally conditional across ontogeny and growth condition (Figures 2 and 3). Interestingly, there were more epistatic interactions identified at Day 17 than at earlier or later growth stages. This is possibly because some interactions were present during earlier developmental stages while others were present during later developmental stages. Day 17 was the age at which early and late patterns appeared to overlap. This suggests a transition in the epistatic network and underlying mechanisms around this time. Interestingly, the strong aliphatic GLS TFs, *MYB28*, *MYB29*, *ANT*, that had minimal single mutant influence on growth, had significant epistatic interactions on plant growth (Figure 2 and 3). Thus, this set of TFs identifies and illustrated an epistatic system influences plant growth depending on age and growth condition. The effects of these TFs on growth are more conditional than the aliphatic GLS effects suggesting that while the traits of growth and defense are both controlled by the epistatic network, they are independent regulatory outputs.

Conditional Epistasis Networks Underlie Plant Growth

To quantify the epistatic effects on plant growth, we used a previously established epistasis value to measure the direction and magnitude of each epistatic interaction (LI *et al.* 2018). Briefly, we subtracted the measured double mutant phenotype from the predicted double mutant phenotype under an additive model. This value was then normalized to the wild type phenotype. This epistasis value was measured for each pair of mutants for all the growth data (Supplemental Data Set 5). The epistasis value will be positive when there is synergistic epistasis and negative for antagonistic epistasis (Figure 3). Previous work showed that epistasis for the short chain GLS (SC GLS), the dominant form of aliphatic GLS, was almost entirely negative/antagonistic (LI *et al.* 2018). Unlike SC GLS, epistasis for growth was a mix of antagonistic and synergistic values that could shift depending upon the conditions and developmental stages. For example, *rap2.6l* was involved in several epistatic interactions that were positive in the LSA growth condition but negative in the CEF growth condition (i.e. *rap2.6/erf9*, etc.); in contrast, epistatic interactions

involving *hmgbd15* had negative interactions in the LSA and positive in the CEF growth conditions (i.e. *ilr3/hmgbd15*); other TF combinations like *myb28/myb29* had similar epistasis across both growth conditions (Figure 4). This argues that this epistatic network of TFs influences growth in both conditions but that the environmental signals in the two conditions permeate differently through the TF network to generate variable growth outputs.

Epistatic Networks Influence Flowering Independent of Tested Environments

To test if these TFs and their network influence reproduction, we measured flowering time in all of the plants from all of the genotypes in the two contrasting chambers, and could show that 12 of the 20 tested TFs significantly influenced flowering (Figure 5). However, unlike growth, the effects on flowering time were almost entirely towards early flowering in both chambers, with only *ANT*, *ILR3* and *ERF9* having an environmental conditionality (Figure 5, and supplemental figure 3). Plotting the epistatic effects for flowering time showed predominantly synergistic epistasis with 18 statistically significant interactions and only 2 interactions having environmental conditionality (Figure 6, A and B). This indicates that the genetic control of flowering time is less influenced by the environmental conditions than are either growth or aliphatic GLS. To further visualize how the epistatic variance was influenced by the network topology, we mapped the epistatic variance for the plant flowering (Figure 6C). Using previously ascribed groupings of the TFs based on their GLS phenotypes, TFs in Group A and B have more significant epistatic interactions partly overlapping with the epistatic interactions of growth phenotype, and TFs with strong main effects on flowering time also have higher genetic variance in their epistatic interactions.

Connections between Defense and Growth

To further explore the connection between plant defense and development, we systemically tested for associations between growth and defense in this data. These TFs predominantly influence the accumulation of SC GLS, and we used this as our quantification for defense (supplemental data set 1) (Li *et al.* 2018). The mutant effects of the 20 TFs on SC GLS, plant growth and flowering time in both chambers were calculated by taking the phenotypic difference between mutant and wild-type and normalized by the wild-type value. We then tested for a relationship between growth and defense by testing for correlations between the mutant effects

using these traits (Figure 7, Supplemental data set 6). In contrast to the expectation if this system was being solely driven by an energetic trade-off model, the TFs' effects on the accumulation of SC GLS and growth/flowering were largely uncorrelated (Figure 7A and B). This was equally true in both the stress and the clean chamber, indicating that the absence of biotic attackers did not illuminate a hidden relationship. As expected, there was a correlation between growth and flowering. Our findings show a highly complex relationship between plant defense and plant growth.

The Connection of Single Mutant and Double Mutant Effects

Given the low correlation between the SC GLS accumulation and plant growth, we proceeded to investigate if there may be any connection between a TF's main effect on a trait and its average epistatic effect on the trait. This allows us to investigate if there is any internal influence of single gene effects on the direction and value of the epistatic value from their double mutants. If there is significant correlation, it would further advance our understanding of internal properties of the epistatic network and revealed underlying quantitative genetic principle governing all the phenotypic changes. To do this, we calculated the average gene epistasis value for each trait for each single TF across all the pairwise combinations. Next, we correlated the TF's estimated single mutant effects to their average gene epistasis value for each phenotype and chamber combinations (Figure 8, Supplemental data set 6). The analysis showed that within all 3 tested traits, there are strong, consistent and negative correlations between a mutation's main and epistatic effects. One possible interpretation of this result is that the genetic background is constraining the results that we have obtained. The prevalence of negative epistasis in the SC GLS phenotype agrees with this possibility. Future work is required to understand if this observation is a general property of this network or is a function of the specific Col-0 accession in which it was conducted.

Discussion

In this study, we tested 20 TF mutants and their 48 double mutants that influence aliphatic GLS accumulation to systemically explore if and how these TFs could significantly influence plant growth and flowering time. 17 of these 20 TFs significantly influence both plant growth and flowering time. Interestingly, the key aliphatic GLS regulators *MYB28* and *MYB29* have

little influence on plant growth and flowering, and what is more, there is no simple mechanistic connection between the TFs' effects on the accumulation of aliphatic SC GLS and growth or flowering. These findings fit with the emerging coordination model whereby the network is dynamic and highly responsive to the specific requirements of a specific environment. We propose that the internal and external signals are coordinated and perceived via connections between these diverse TFs. These connections create a decision matrix whereby growth and aliphatic GLS are interpreted and coordinated. Independent connections to growth and aliphatic GLS then proceed from this matrix to maximize plant fitness in a given environmental setting. (Figure 9). Further, this suggests that TF networks provide an unappreciated potential to fine-tune both growth and defense to optimize modern agriculture.

Growth and Defense vs Coordination

The canonical model for plant growth and plant defense is a trade-off model, which treats plant growth and defense as two competing biological processes under the assumption that the acquisition of elements and energy are limiting, a zero sum game. A complementary hypothesis is that growth and defense are two separable outputs of the plant's regulatory system that must be coordinated depending on the specific environment. The analysis of the phenotypes in this TF collection and epistatic network in aliphatic GLS pathway supported the existence of the coordination model. The complex interactions between growth and defense depended on the specific perturbed TF, the environment and their epistatic effects. There was no consistent evidence of any negative relationship between the accumulation of the SC GLS defense metabolites and any measurement of growth. This suggests that the TFs collectively make growth and defense decisions in a coordinated fashion in our case study, and the final growth and defense phenotypes are the outcomes from this decision process. Future work is required to test if this decision process is truly structured to shape both growth and defense in a way that always maximizes the individual's fitness potential in their ecological niche. This suggests that future experiments need to incorporate more complex regulatory relationships to truly understand how growth and defense are related in the field.

Using Transcription Factors to Tune and Optimize Growth and Defense

Putative costs of plant defenses on growth have been intensively researched, and recent findings are suggesting that it is possible to promote one without sacrificing the other (CAMPOS *et al.* 2016; WANG *et al.* 2018). Our current study further brightens the future potential to optimize plant growth and defense through TF manipulation. Specifically, we found that there are a vast array of potential TFs that can be identified and potentially used to manipulate plant growth and defense. In our system, mutations in more than half of the tested TFs could significantly promote plant growth and defense together across diverse environmental conditions. Critically, this ability to promote both defense and growth is highly conditional on the specific environment in which the phenotypes are being measured. If this is true in other genes and TFs involving plant growth and defense, it raises the importance of studying plants' response to genetic manipulation under different growth conditions, which is especially relevant and pertinent to crop breeding efforts in changing climate and environmental stresses. To fully interrogate this potential, future studies are needed that involve larger collections of TFs and epistatic interactions across even more diverse environments to further understand the coordination between growth and defense across fluctuating environments.

MATERIALS AND METHODS

Plant materials and growth conditions

The *Arabidopsis thaliana* T-DNA insertion lines of the 20 TFs were ordered from Arabidopsis Biological Resource Center (SUSSMAN *et al.* 2000; ALONSO *et al.* 2003) and homozygous lines were validated in previous studies (SØNDERBY *et al.* 2010a; LI *et al.* 2014). The 47 double mutants were generated and validated and planted in previous study (LI *et al.* 2018). Briefly, the Arabidopsis plants were grown in two independent chambers with 16-h light at 100- to 120-µEi light intensity with temperature set at a continuous 22ºC. The two growth chambers were set to similar abiotic environments but contain dramatically different biotic environments, one pest free, clean CEF as a typical lab growth condition, and one with an endogenous pest population, herbivore LSA mimicking the nature growth condition. Seeds were imbibed in water at 4°C for 3 days and sown into Sunshine Mix (Sun Gro Horticulture). Seedlings were thinned to one plant per pot (6cm x 5cm) at 7 d after planting. For each experiment, at least 8 replicates of Col-0, single and double were planted using a randomized complete block design. Each flat had one plant per genotype leading to eight flats per replication. This experiment was conducted

independently in the clean CEF and herbivore LSA chamber to generate a minimum of 16 biological repeats in total for most of the genotypes.

Flowering time and plant growth measurement

All the plants were checked daily, and the day was recorded for each of the plants when the first flower opened. The flowering time was measured as how many days it takes for the plant to have the first flower opened. All the plants were taken photos from day 9 to day 27 when some of the early flowering lines in stress chamber started to flower. The circling area of the rosette of each of the plant in each growth condition was manually measured by Image J across the days. The area was used as an indicator of the plant size. The plant flowering time and plant sizes were normalized with the number of Col-0, and further visualized using the iheatmapr package in R software (R DEVELOPMENT CORE TEAM 2014).

Statistics

To test for epistasis of the TFs in controlling plant development, the flowering time and plant growth for each epistatic combination were separately analyzed by ANOVA using a general linear model with lmerTest in R (KUZNETSOVA *et al.* 2017). The following model was used to test for the epistasis for the flowering time and growth phenotypes in the double mutants, with each double mutant having both single mutants and wild type grown concurrently: $y_{abc} = \mu + A_a + B_b + Ch_c + A_a x B_b + A_a x Ch_c + B_b x Ch_c + A_a x B_b x Ch_c + \varepsilon_{abc}$, where ε_{abc} is the error term and is assumed to be normally distributed with mean 0 and variance σ_ε^2. In this model, y_{abc} denotes the plant flowering and growth data in each plant, Genotype A represents the presence or absence of a T-DNA insert in one TF gene (WT versus mutant of locus A), and Genotype *B* represents the presence or absence of a T-DNA insert in another TF gene (WT versus mutant of locus B) in the double mutant from Chamber Ch_c (Clean CEF chamber or herbivore LSA Chamber). The ANOVA table, least-square (LS) means and standard error for each genotype x treatment combinations were obtained with emmeans package in R (SEARLE *et al.* 1980). The type III sums-of-squares from this model were used to calculate the variance and percent variance attributable to each term in the model. For the percent variance, this was calculated by comparing to the total variance in the model as the denominator. All network representations were generated using Cytoscape.v2.8.3 (SHANNON *et al.* 2003).

Calculation of epistasis value

To study the effect of epistasis, we use epistasis value to describe the direction and strength of the epistasis by normalizing the difference of observed double mutant phenotype versus the predicted double mutant phenotype, assuming additivity of the single mutants, then normalized to the wild type as reported before (SEGRE *et al.* 2005; LI *et al.* 2018).The phenotype for WT was set as w, mutant TFa as a, mutant TFb as b, and double mutant TFa/TFb as ab. The Epistasis Value is calculated as (ab - (w + (a-w) + (b-w))/w). If the epistasis value is positive, this shows evidence for synergistic epistasis, while antagonistic epistasis is reflected in negative values. The larger the epistasis value, the stronger the epistasis effects. The Epistasis Value were further visualized using the iheatmapr package in R software (R DEVELOPMENT CORE TEAM 2014).

Acknowledgements

Funding for this work was provided by the NSF awards IOS 1655810 and 1547796 to DJK, the USDA National Institute of Food and Agriculture, Hatch project number CA-D-PLS-7033-H to DJK and by the Danish National Research Foundation (DNRF99) grant to DJK. SMB was partially funded by an HHMI Faculty Scholar Fellowship.

References:

Agrawal, A. A., 2011a Current trends in the evolutionary ecology of plant defence. Functional Ecology 25: 420-432.

Agrawal, A. A., 2011b New synthesis-trade-offs in Chemical Ecology. Journal of Chemical Ecology 37: 230-231.

Almeida-Cortez, J. S., B. Shipley and J. T. Arnason, 1999 Do plant species with high relative growth rates have poorer chemical defences? Functional Ecology 13: 819-827.

Alonso, J. M., A. N. Stepanova, T. J. Leisse, C. J. Kim, H. M. Chen *et al.*, 2003 Genome-wide Insertional mutagenesis of *Arabidopsis thaliana*. Science 301: 653-657.

Bekaert, M., P. P. Edger, C. M. Hudson, J. C. Pires and G. C. Conant, 2012 Metabolic and evolutionary costs of herbivory defense: Systems biology of glucosinolate synthesis. New Phytologist 196: 596-605.

Beran, F., Y. Pauchet, G. Kunert, M. Reichelt, N. Wielsch *et al.*, 2014 Phyllotreta striolata flea beetles use host plant defense compounds to create their own glucosinolate-myrosinase system. Proceedings of the National Academy of Sciences of the United States of America 111: 7349-7354.

Bergelson, J., and C. B. Purrington, 1996 Surveying patterns in the cost of resistance in plants. American Naturalist 148: 536-558.

Bidart-Bouzat, M. G., and D. J. Kliebenstein, 2008 Differential levels of insect herbivory in the field associated with genotypic variation in glucosinolates in *Arabidopsis thaliana*. Journal of Chemical Ecology 34: 1026-1037.

Burow, M., B. A. Halkier and D. J. Kliebenstein, 2010 Regulatory networks of glucosinolates shape *Arabidopsis thaliana* fitness. Curr Opin Plant Biol 13: 348-353.

Campos, M. L., Y. Yoshida, I. T. Major, D. de Oliveira Ferreira, S. M. Weraduwage *et al.*, 2016 Rewiring of jasmonate and phytochrome B signalling uncouples plant growth-defense tradeoffs. Nat Commun 7: 12570.

de Lucas, M., L. Pu, G. Turco, A. Gaudinier, A. K. Morao *et al.*, 2016 Transcriptional Regulation of Arabidopsis Polycomb Repressive Complex 2 Coordinates Cell-Type Proliferation and Differentiation. Plant Cell 28: 2616-2631.

Falk, K. L., J. Kastner, N. Bodenhausen, K. Schramm, C. Paetz *et al.*, 2014 The role of glucosinolates and the jasmonic acid pathway in resistance of Arabidopsis thaliana against molluscan herbivores. Mol Ecol 23: 1188-1203.

Fan, M., M. Y. Bai, J. G. Kim, T. Wang, E. Oh *et al.*, 2014 The bHLH transcription factor HBI1 mediates the trade-off between growth and pathogen-associated molecular pattern-triggered immunity in Arabidopsis. Plant Cell 26: 828-841.

Hemm, M. R., M. O. Ruegger and C. Chapple, 2003 The Arabidopsis ref2 mutant is defective in the gene encoding CYP83A1 and shows both phenylpropanoid and glucosinolate phenotypes. Plant Cell 15: 179-194.

Huot, B., J. Yao, B. L. Montgomery and S. Y. He, 2014 Growth-defense tradeoffs in plants: a balancing act to optimize fitness. Mol Plant 7: 1267-1287.

Jiao, Y., Y. Wang, D. Xue, J. Wang, M. Yan *et al.*, 2010 Regulation of OsSPL14 by OsmiR156 defines ideal plant architecture in rice. Nat Genet 42: 541-544.

Joseph, B., J. A. Corwin, T. Zuest, B. Li, M. Iravani *et al.*, 2013 Hierarchical nuclear and cytoplasmic genetic architectures for plant growth and defense within *Arabidopsis*. Plant Cell 25: 1929-1945.

Karban, R., and I. T. Baldwin, 1997 *Induced Responses to Herbivory*. University of Chicago Press, Chicago, IL, USA.

Kerwin, R., J. Feusier, J. Corwin, M. Rubin, C. Lin *et al.*, 2015 Natural genetic variation in Arabidopsis thaliana defense metabolism genes modulates field fitness. Elife 4.

Kerwin, R. E., J. Feusier, A. Muok, C. Lin, B. Larson *et al.*, 2017 Epistasis x environment interactions among Arabidopsis thaliana glucosinolate genes impact complex traits and fitness in the field. New Phytol 215: 1249-1263.

Kerwin, R. E., J. M. Jiménez-Gómez, D. Fulop, S. L. Harmer, J. N. Maloof *et al.*, 2011 Network quantitative trait loci mapping of circadian clock outputs identifies metabolic pathway-to-clock linkages in Arabidopsis. Plant Cell 23: 471-485.

Kliebenstein, D., D. Pedersen, B. Barker and T. Mitchell-Olds, 2002 Comparative analysis of quantitative trait loci controlling glucosinolates, myrosinase and insect resistance in *Arabidopsis thaliana*. Genetics 161: 325-332.

Kliebenstein, D. J., 2016 False idolatry of the mythical growth versus immunity tradeoff in molecular systems plant pathology. Physiological and Molecular Plant Pathology 95.

Kliebenstein, D. J., J. Kroymann, P. Brown, A. Figuth, D. Pedersen *et al.*, 2001 Genetic control of natural variation in *Arabidopsis thaliana* glucosinolate accumulation. Plant Physiol 126: 811-825.

Koricheva, J., 2002 Meta-analysis of sources of variation in fitness costs of plant antiherbivore defenses. Ecology 83: 176-190.

Kos, M., B. Houshyani, R. Wietsma, P. Kabouw, L. E. Vet *et al.*, 2012 Effects of glucosinolates on a generalist and specialist leaf-chewing herbivore and an associated parasitoid. Phytochemistry 77: 162-170.

Kuznetsova, A., P. B. Brockhoff and R. H. B. Christensen, 2017 lmerTest Package: Tests in Linear Mixed Effects Models. 2017 82: 26 %J Journal of Statistical Software.

Lambrix, V., M. Reichelt, T. Mitchell-Olds, D. J. Kliebenstein and J. Gershenzon, 2001 The Arabidopsis epithiospecifier protein promotes the hydrolysis of glucosinolates to nitriles and influences *Trichoplusia ni* herbivory. Plant Cell 13: 2793-2807.

Li, B., A. Gaudinier, M. Tang, M. Taylor-Teeples, N. T. Nham *et al.*, 2014 Promoter-based integration in plant defense regulation. Plant physiology 166: 1803-1820.

Li, B., M. Tang, A. Nelson, H. Caligagan, X. Zhou *et al.*, 2018 Network-Guided Discovery of Extensive Epistasis between Transcription Factors Involved in Aliphatic Glucosinolate Biosynthesis. Plant Cell 30: 178-195.

Lozano-Duran, R., A. P. Macho, F. Boutrot, C. Segonzac, I. E. Somssich *et al.*, 2013 The transcriptional regulator BZR1 mediates trade-off between plant innate immunity and growth. Elife 2: e00983.

Pajerowska-Mukhtar, K. M., W. Wang, Y. Tada, N. Oka, C. L. Tucker *et al.*, 2012 The HSF-like Transcription Factor TBF1 Is a Major Molecular Switch for Plant Growth-to-Defense Transition. Current Biology 22: 103-112.

Paul-Victor, C., T. Züst, M. Rees, D. J. Kliebenstein and L. A. Turnbull, 2010 A new method for measuring relative growth rate can uncover the costs of defensive compounds in Arabidopsis thaliana. New Phytologist 187: 1102-1111.

R Development Core Team, 2014 R: A Language and Environment for Statistical Computing, pp., edited by R. F. f. S. Computing, Vienna.

Schlaeppi, K., N. Bodenhausen, A. Buchala, F. Mauch and P. Reymond, 2008 The glutathione-deficient mutant pad2-1 accumulates lower amounts of glucosinolates and is more susceptible to the insect herbivore Spodoptera littoralis. Plant Journal 55: 774-786.

Searle, S. R., F. M. Speed and G. A. Milliken, 1980 Population Marginal Means in the Linear Model: An Alternative to Least Squares Means. The American Statistician 34: 216-221.

Segre, D., A. Deluna, G. M. Church and R. Kishony, 2005 Modular epistasis in yeast metabolism. Nat Genet 37: 77-83.

Shannon, P., A. Markiel, O. Ozier, N. S. Baliga, J. T. Wang *et al.*, 2003 Cytoscape: a software environment for integrated models of biomolecular interaction networks. Genome Res 13: 2498-2504.

Singh, K., R. C. Foley and L. Onate-Sanchez, 2002 Transcription factors in plant defense and stress responses. Curr Opin Plant Biol 5: 430-436.

Sønderby, I. E., M. Burow, H. C. Rowe, D. J. Kliebenstein and B. A. Halkier, 2010a A complex interplay of three R2R3 MYB transcription factors determines the profile of aliphatic glucosinolates in Arabidopsis. Plant physiology 153: 348-363.

Sønderby, I. E., F. Geu-Flores and B. A. Halkier, 2010b Biosynthesis of glucosinolates–gene discovery and beyond. Trends in plant science 15: 283-290.

Sønderby, I. E., B. G. Hansen, N. Bjarnholt, C. Ticconi, B. A. Halkier *et al.*, 2007 A systems biology approach identifies a R2R3 MYB gene subfamily with distinct and overlapping functions in regulation of aliphatic glucosinolates. PLoS One 2: e1322.

Sussman, M. R., R. M. Amasino, J. C. Young, P. J. Krysan and S. Austin-Phillips, 2000 The Arabidopsis knockout facility at the University of Wisconsin-Madison. Plant Physiology 124: 1465-1467.

Wang, J., L. Zhou, H. Shi, M. Chern, H. Yu *et al.*, 2018 A single transcription factor promotes both yield and immunity in rice. Science 361: 1026-1028.

Wentzell, A. M., and D. J. Kliebenstein, 2008 Genotype, age, tissue, and environment regulate the structural outcome of glucosinolate activation. Plant Physiol 147: 415-428.

Zalucki, M. P., J. M. Zalucki, L. E. Perkins, K. Schramm, D. G. Vassao *et al.*, 2017 A Generalist Herbivore Copes with Specialized Plant Defence: the Effects of Induction and Feeding by Helicoverpa

armigera (Lepidoptera: Noctuidae) Larvae on Intact Arabidopsis thaliana (Brassicales) Plants. J Chem Ecol 43: 608-616.
Zust, T., and A. A. Agrawal, 2017 Trade-Offs Between Plant Growth and Defense Against Insect Herbivory: An Emerging Mechanistic Synthesis. Annu Rev Plant Biol 68: 513-534.
Züst, T., B. Joseph, K. K. Shimizu, D. J. Kliebenstein and L. A. Turnbull, 2011 Using knockout mutants to reveal the growth costs of defensive traits. Proceedings of the Royal Society B-Biological Sciences 278: 2598-2603.

Figure Legend

Figure 1. The Effects of the 20 TFs on Plant Growth

The heatmap displays the fold change of plant size in single mutants, from day 9 to day 27, in comparison to Col-0 in both the clean CEF chamber and herbivore LSA chamber. Red shows increased plant size and blue decreased plant size. The columns on the right display the statistical significance (purple, significant $p< 0.05$; gray, not significant) for each term in the statistical model as listed at the bottom. Specific framed genotypes have mean phenotypes shown for reference in Supplemental Figure 1.

Figure 2. Epistatic networks for representative growth days

Connectivity plots of epistatic interactions between TF genes are shown. The TFs are laid out in the network based on their effect on aliphatic GLS accumulation. Solid lines show that the TF x TF interaction term was significant while dotted shows significant Treatment x TF x TF interaction in the statistical model. A line of arrows shows that the interaction was conditional on both treatment and tissue. The color of the node indicates which main effect terms are significant for the individual TFs; sky blue indicates only a TF main effect, green indicates only a treatment x TF interaction, yellow indicates both TF and treatment x TF.

A-E: Shows the network significances on Day 9, 13, 17, 21, and 25.

F: Visualization of individual epistatic variance components within the genetic network for day25. The width of the line connecting 2 TFs is proportional to the variance linked with the TF x TF term for that specific interaction.

Figure 3. Epistatic effects on plant growth

Epistasis values were calculated for all pairwise TF combinations from day 9 to day 27 in each treatment condition. These values are plotted in a heatmap for all pairwise mutant combinations.

The genotypes are clustered using hierarchical clustering and labeled to the right of the diagram. The columns to the right of the heat map show which epistatic interaction term is significant (purple) or not significant (gray) ($P < 0.05$). Specific framed genotypes have mean phenotypes shown for reference in Figure 4.

Figure 4. Representative epistatic growth phenotypes

The average rosette size on day 15 for the corresponding genotypes from the clean CEF and herbivore LSA chambers are plotted. Different letters indicate genotypes with significantly different plant sizes. ($P < 0.05$ using post-hoc Tukey's test). SE is shown with 8 samples across two experiments for each genotype. Day 15 was chosen to provide a common date across which to illustrate key differences.

(A) Rosette size of single and double mutants of *rap2.6l* and *erf9*

(B) Rosette size single and double mutants of *ilr3* and *hmgbd15*

(C) Rosette size single and double mutants of *myb28* and *myb29*

Figure 5. TF Effects on Flowering Time

The heatmap displays the fold change of flowering time in the single mutants compared with Col-0 in both clean CEF chamber and herbivore LSA chamber. Red shows increased flowering time and blue decreased flowering time. The columns on the right display the statistical significance (purple, significant $p< 0.05$; gray, not significant) for each term in the statistical model as listed at the bottom.

Figure 6. Epistatic network and flowering time effects

A: Epistasis values were calculated for all pairwise combinations individually in both treatment conditions and plotted in the heatmap. The genotypes are clustered using hierarchical clustering and labeled to the right of the diagram. The columns to the right of the heatmap show which epistatic interaction term is significant (purple) or not significant (grey) ($P < 0.05$).

B: A representation of the significant epistatic networks is shown for flowering time. Solid lines show that only the TF x TF interaction term was significant and a dotted line shows where there was a significant chamber x TF x TF interaction. The node color indicates which main effect

terms are significant for the individual TFs; sky blue indicates only a TF main effect, green indicates only a chamber x TF interaction, yellow indicates both TF and chamber x TF.
C: Visualization of individual epistatic variance components within the genetic network for flowering time. The width of the line connecting 2 TFs is proportional to the variance linked with the TF x TF term for that specific interaction.

Figure 7. Lack of relationship between mutant effects on defense and growth.
The main additive effect of the TF mutants in herbivore LSA chamber were selected to illustrate the absence of a relationship between growth, flowering time and SC GLS. The predicted linear tread line and the statistical test results are shown.
A: Comparison of gene effects on SC GLS and flowering time ($r = -0.006$, $p = 0.980$). This result was unaffected by the presence or absence of the outlier point for SC GLS.
B: Comparison of gene effects on SC GLS and growth ($r = 0.131$, $p = 0.583$). This result was unaffected by the presence or absence of the outlier point for SC GLS.
C: Comparison of gene effects on flowering time and growth ($r = -0.867$, $p < 0.001$).

Figure 8. Relationship of the main and epistatic effects for TF genes
The average epistatic effect of a TF across all its pairs in the herbivore LSA chamber was calculated and compared to the TFs main effects for SC GLS, flowering time and plant size on Day 17. The predicted linear tread line and the statistical test results are shown.
A: Comparison of main gene and average epistatic gene effects on SC GLS ($r = -0.610$, $p = 0.004$).
B: Comparison of main gene and average epistatic gene effects on flowering time ($r = -0.732$, $p < 0.001$).
C: Comparison of main gene and average epistatic gene effects on flowering time on growth ($r = -0.841$, $p < 0.001$).

Figure 9. Proposed model for TF coordination of plant development and aliphatic GLS based plant defense
External environmental and internal developmental signals are coordinately perceived via a group of TFs. Direct and indirect connections between these TFs allow for a coordinated

response to these complex signals. A theoretically cohesive response is then transmitted to growth and defense via separate outputs from this network.

Supplemental Figure 1. Representative plant growth phenotypes in single TF mutants
Rosette sizes on day 15 for the corresponding genotypes are shown in the clean CEF and herbivore LSA chambers. Different letters indicate genotypes with significantly different plant sizes. ($P < 0.05$ using post-hoc Tukey's test). SE is shown with 8 samples across two experiments for each genotype.
(A) *cbf4*
(B) *abf4*
(C) *ilr3*

Supplemental Figure 2. Dynamic Mutant Effects on Plant Growth
Rosette growth of specific mutations in comparison to Col-0 is shown across time. Col-0 is shown as a solid line while mutants are the dashed line. Data from the CEF clean chamber are shown as black lines data from the herbivore LSA chamber are red lines.
(A) *cbf4*
(B) *abf4*
(C) *ilr3*

Supplemental Figure 3. Representative flowering time phenotypes in single TF mutants
Flowering time in specific genotypes is shown for both the clean CEF and herbivore LSA chamber. Different letters indicate genotypes with significantly different flowering time. ($P < 0.05$ using post-hoc Tukey's test). SE is shown with 16 samples across two experiments for each genotype.
(A) *zfp7*
(B) *ant*
(C) *ilr3*

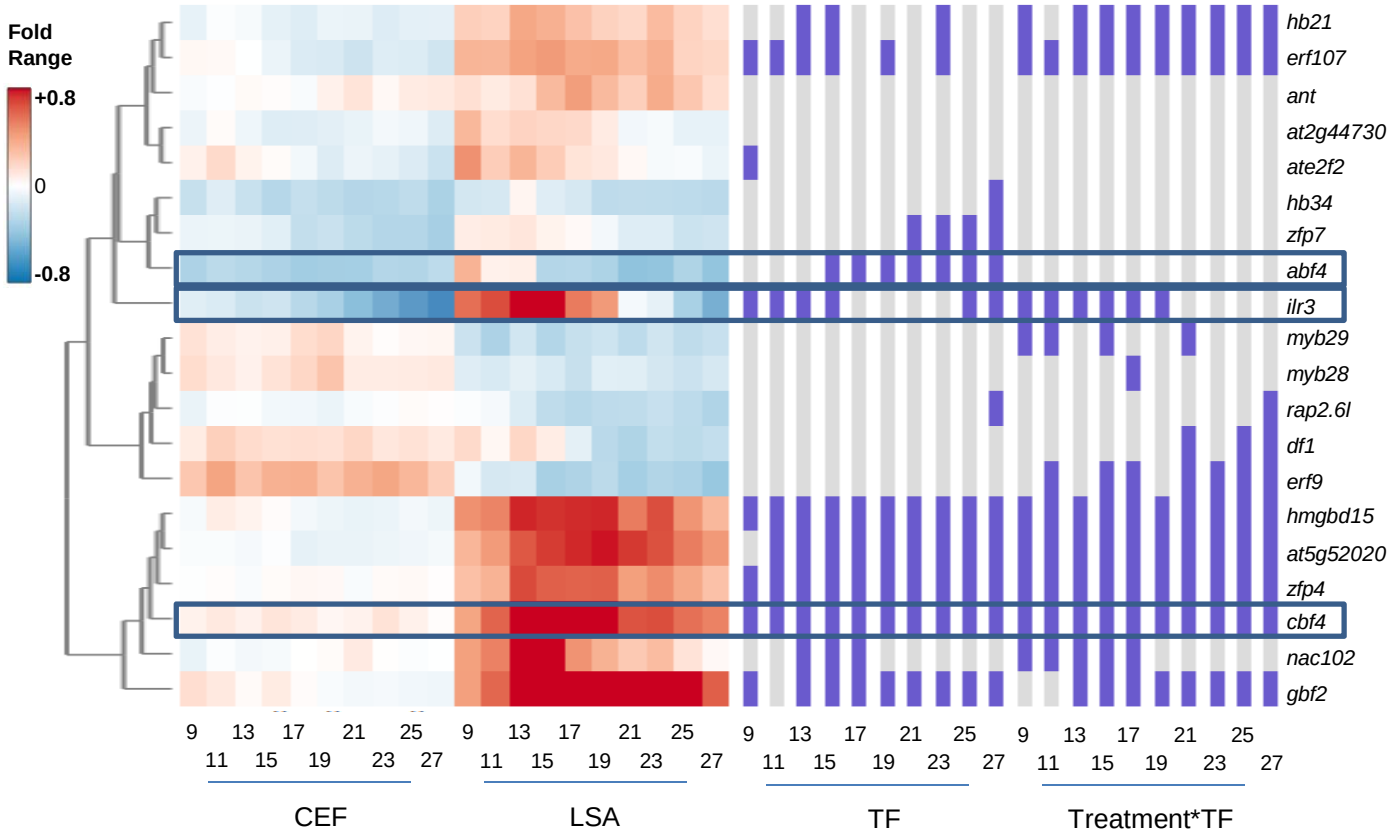
Fold Range
+0.8
0
-0.8
hb21
erf107
ant
at2g44730
ate2f2
hb34
zfp7
abf4
ilr3
myb29
myb28
rap2.6l
df1
erf9
hmgbd15
at5g52020
zfp4
cbf4
nac102
gbf2
9 13 17 21 25
11 15 19 23 27
CEF
LSA
TF
Treatment*TF

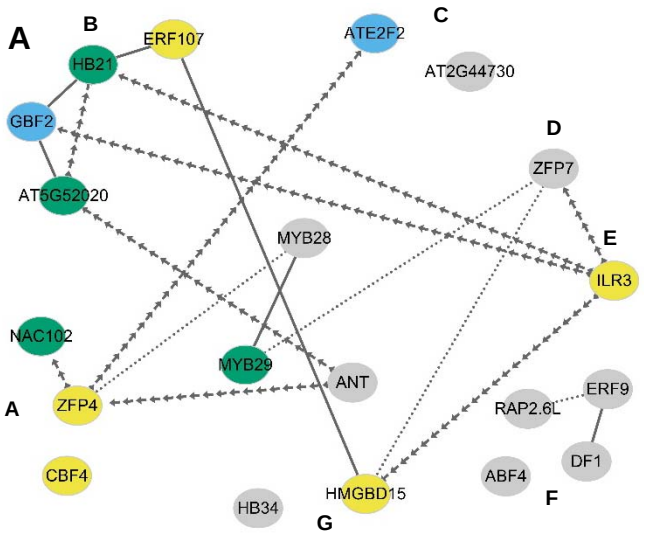

Day 9

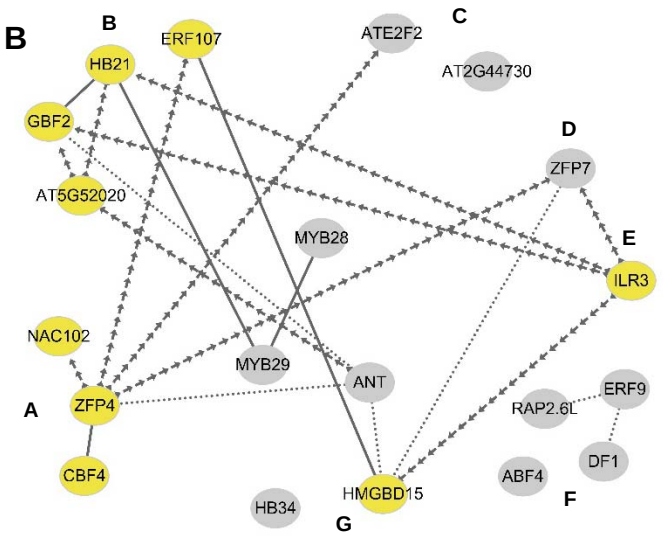

Day 13

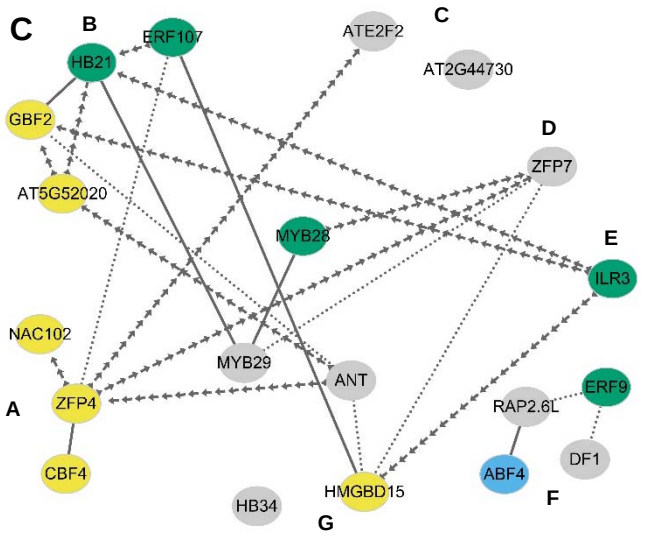

Day 17

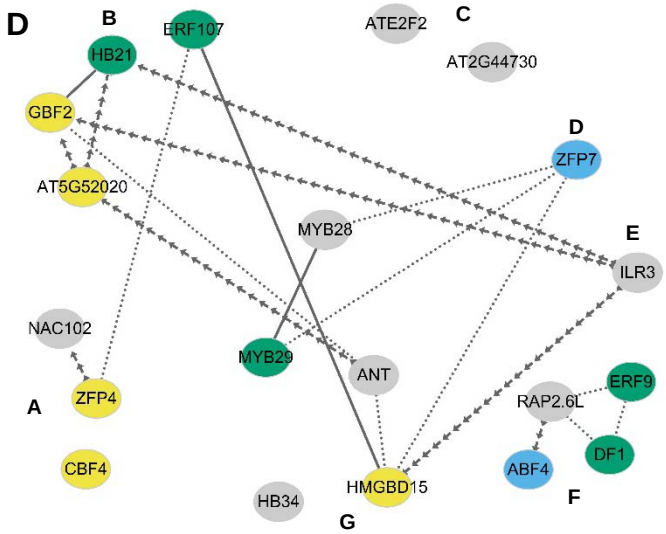

Day 21

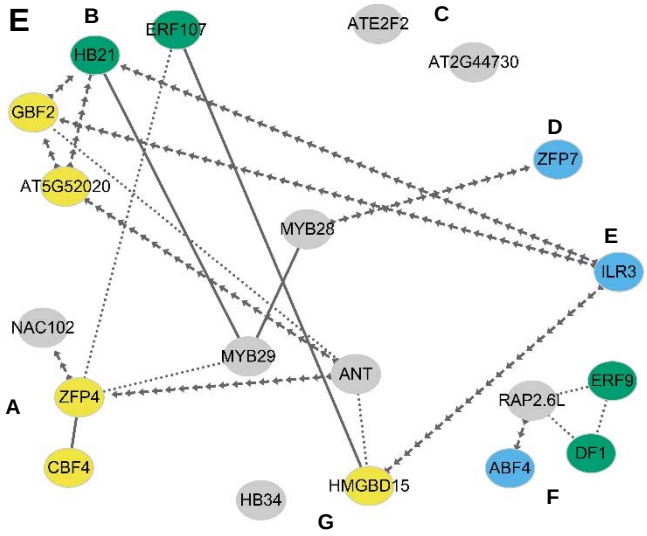

Day 25

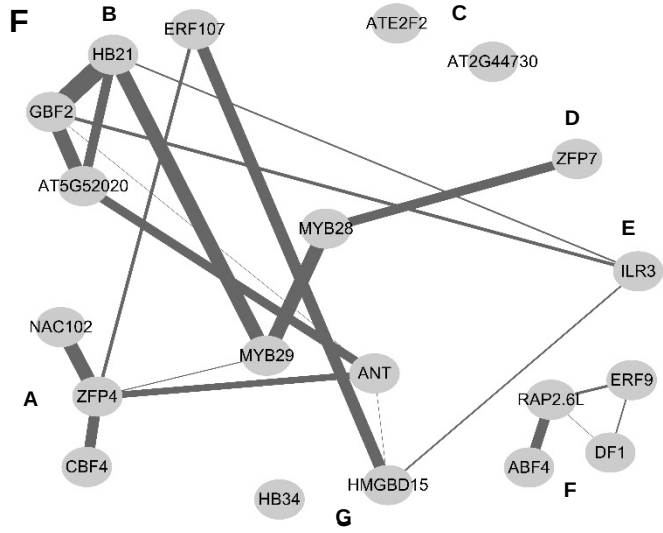

Day 25

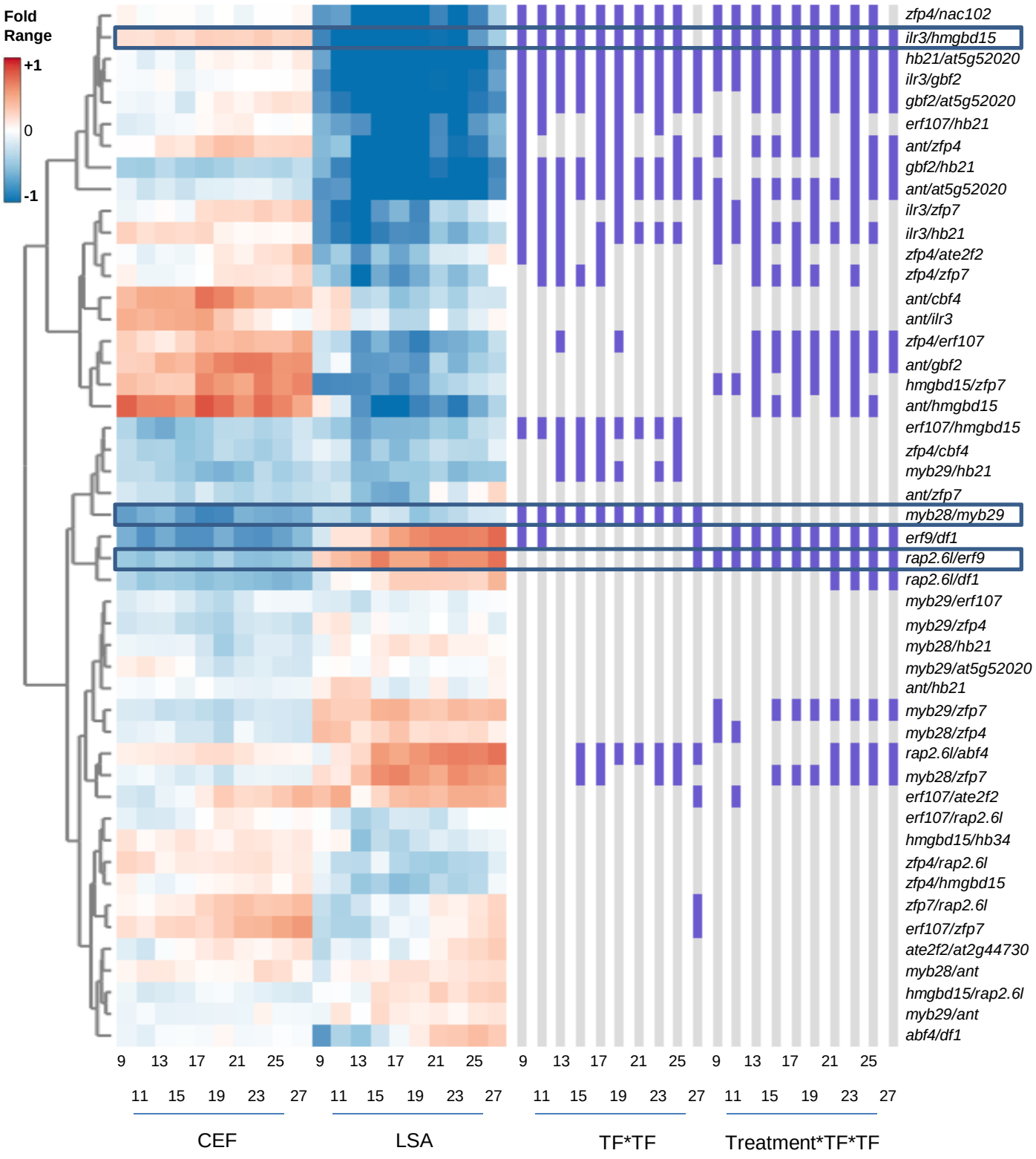
Fold Range
+1
0
-1
zfp4/nac102
ilr3/hmgbd15
hb21/at5g52020
ilr3/gbf2
gbf2/at5g52020
erf107/hb21
ant/zfp4
gbf2/hb21
ant/at5g52020
ilr3/zfp7
ilr3/hb21
zfp4/ate2f2
zfp4/zfp7
ant/cbf4
ant/ilr3
zfp4/erf107
ant/gbf2
hmgbd15/zfp7
ant/hmgbd15
erf107/hmgbd15
zfp4/cbf4
myb29/hb21
ant/zfp7
myb28/myb29
erf9/df1
rap2.6l/erf9
rap2.6l/df1
myb29/erf107
myb29/zfp4
myb28/hb21
myb29/at5g52020
ant/hb21
myb29/zfp7
myb28/zfp4
rap2.6l/abf4
myb28/zfp7
erf107/ate2f2
erf107/rap2.6l
hmgbd15/hb34
zfp4/rap2.6l
zfp4/hmgbd15
zfp7/rap2.6l
erf107/zfp7
ate2f2/at2g44730
myb28/ant
hmgbd15/rap2.6l
myb29/ant
abf4/df1
9 13 17 21 25 9 13 17 21 25 9 13 17 21 25 9 13 17 21 25
11 15 19 23 27 11 15 19 23 27 11 15 19 23 27 11 15 19 23 27
CEF
LSA
TF*TF
Treatment*TF*TF

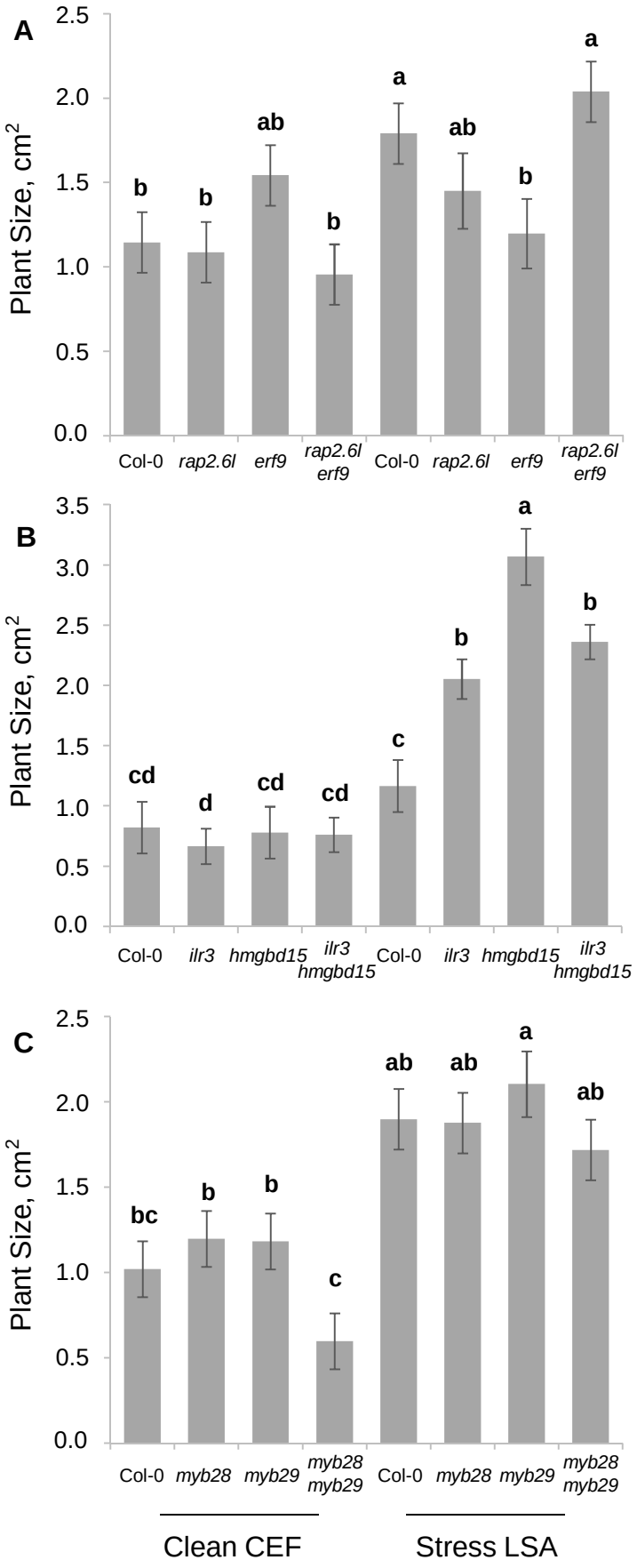
A
Plant Size, cm2
2.5
2.0
1.5
1.0
0.5
0.0
b
b
ab
b
a
ab
b
a
Col-0
rap2.6l
erf9
rap2.6l erf9
Col-0
rap2.6l
erf9
rap2.6l erf9
B
Plant Size, cm2
3.5
3.0
2.5
2.0
1.5
1.0
0.5
0.0
cd
d
cd
cd
c
b
a
b
Col-0
ilr3
hmgbd15
ilr3 hmgbd15
Col-0
ilr3
hmgbd15
ilr3 hmgbd15
C
Plant Size, cm2
2.5
2.0
1.5
1.0
0.5
0.0
bc
b
b
c
ab
ab
a
ab
Col-0
myb28
myb29
myb28 myb29
Col-0
myb28
myb29
myb28 myb29
Clean CEF
Stress LSA

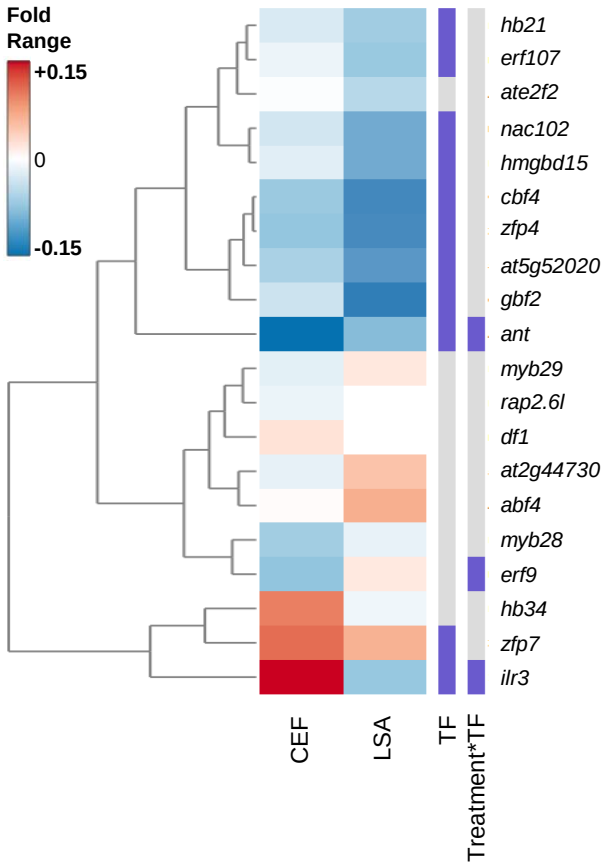
Fold
Range
+0.15
0
-0.15
hb21
erf107
ate2f2
nac102
hmgbd15
cbf4
zfp4
at5g52020
gbf2
ant
myb29
rap2.6l
df1
at2g44730
abf4
myb28
erf9
hb34
zfp7
ilr3
CEF
LSA
TF
Treatment*TF

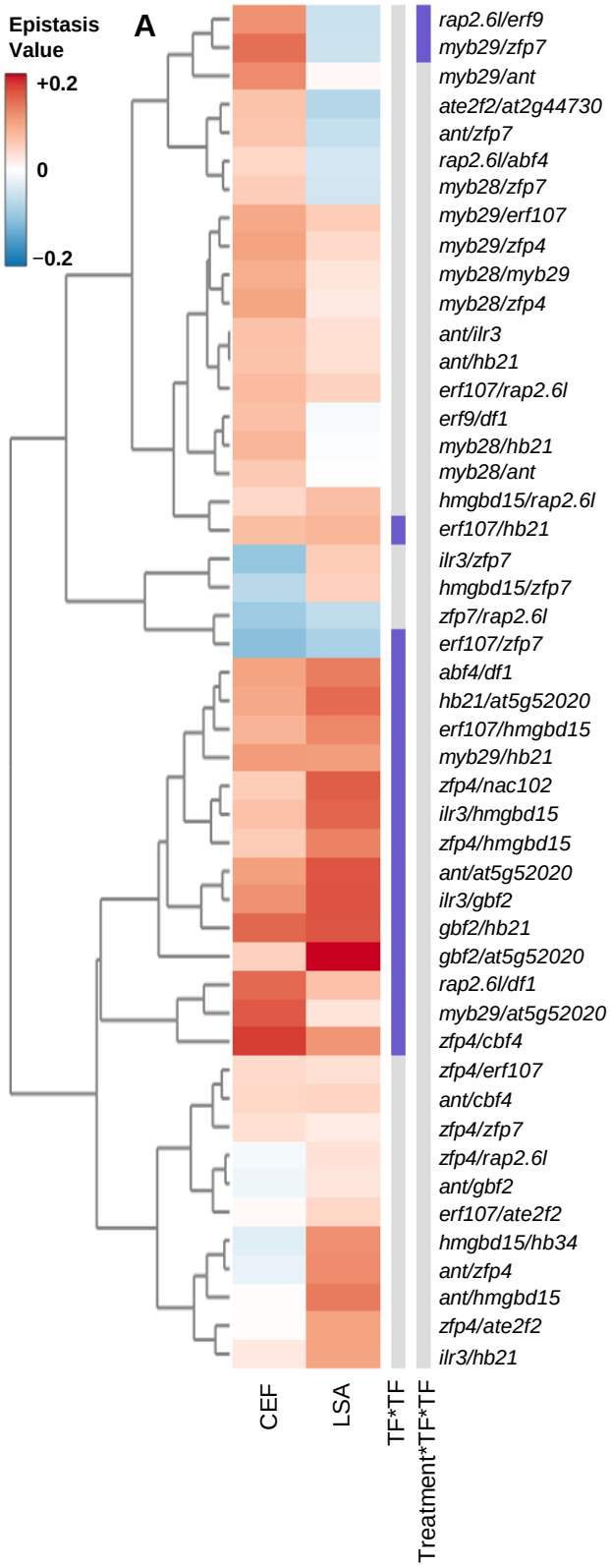
A
Epistasis Value
+0.2
0
−0.2
rap2.6l/erf9
myb29/zfp7
myb29/ant
ate2f2/at2g44730
ant/zfp7
rap2.6l/abf4
myb28/zfp7
myb29/erf107
myb29/zfp4
myb28/myb29
myb28/zfp4
ant/ilr3
ant/hb21
erf107/rap2.6l
erf9/df1
myb28/hb21
myb28/ant
hmgbd15/rap2.6l
erf107/hb21
ilr3/zfp7
hmgbd15/zfp7
zfp7/rap2.6l
erf107/zfp7
abf4/df1
hb21/at5g52020
erf107/hmgbd15
myb29/hb21
zfp4/nac102
ilr3/hmgbd15
zfp4/hmgbd15
ant/at5g52020
ilr3/gbf2
gbf2/hb21
gbf2/at5g52020
rap2.6l/df1
myb29/at5g52020
zfp4/cbf4
zfp4/erf107
ant/cbf4
zfp4/zfp7
zfp4/rap2.6l
ant/gbf2
erf107/ate2f2
hmgbd15/hb34
ant/zfp4
ant/hmgbd15
zfp4/ate2f2
ilr3/hb21
CEF
LSA
TF*TF
Treatment*TF*TF

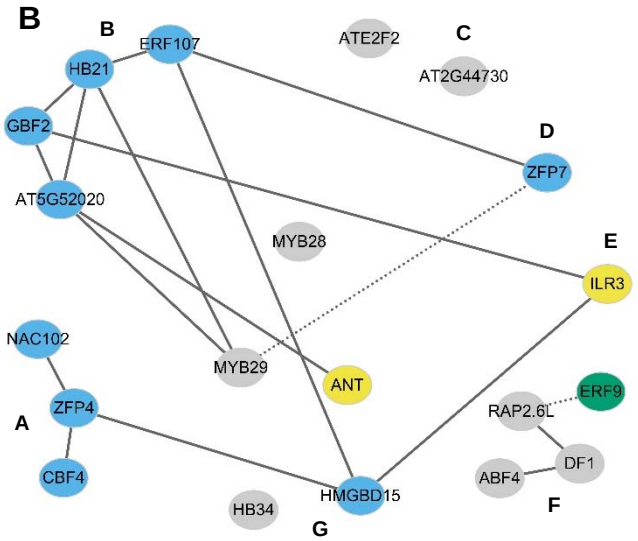
B
B
ERF107
HB21
ATE2F2
C
AT2G44730
GBF2
D
ZFP7
AT5G52020
MYB28
E
ILR3
NAC102
MYB29
ANT
ERF9
ZFP4
RAP2.6L
A
DF1
CBF4
ABF4
HMGBD15
HB34
F
G

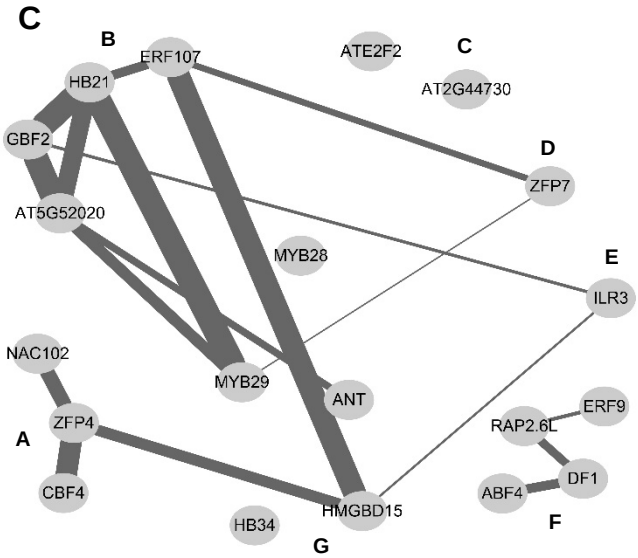
C
B
ERF107
HB21
ATE2F2
C
AT2G44730
GBF2
D
ZFP7
AT5G52020
MYB28
E
ILR3
NAC102
MYB29
ANT
ERF9
ZFP4
RAP2.6L
A
DF1
CBF4
ABF4
HMGBD15
HB34
F
G

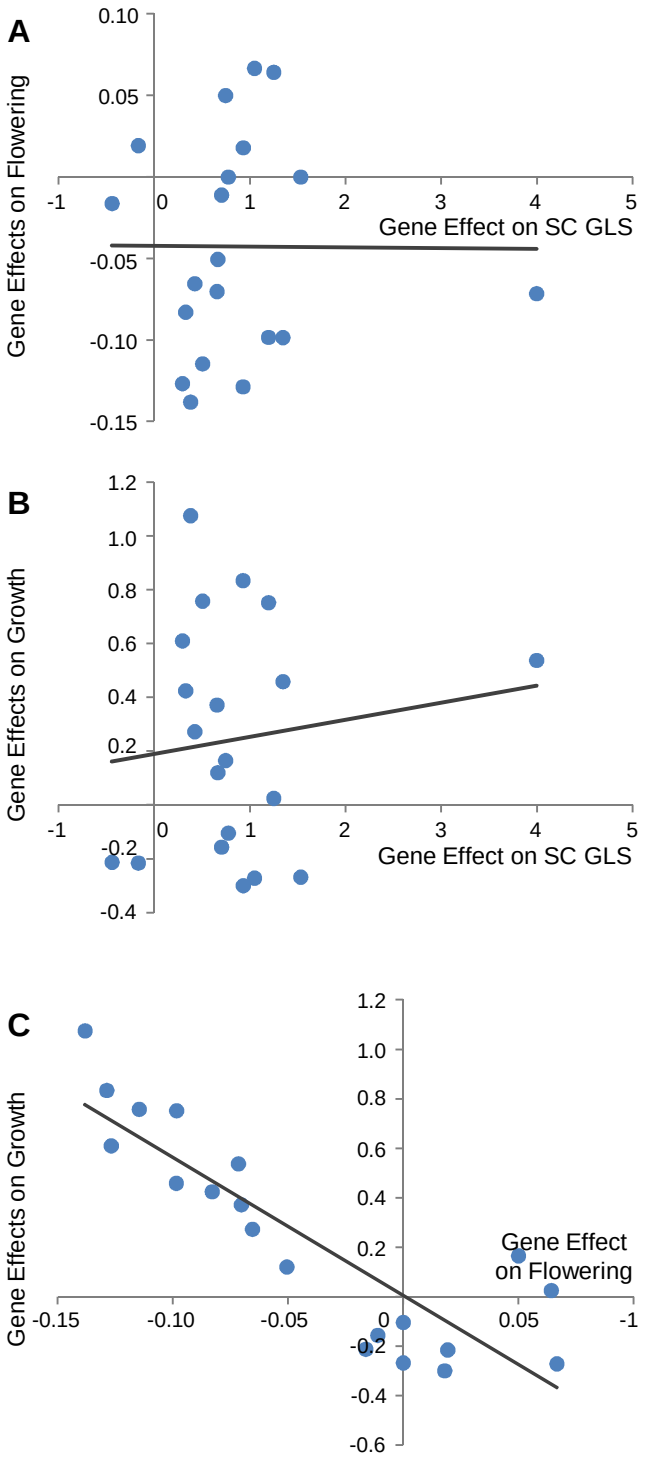
A
Gene Effects on Flowering
0.10
0.05
-0.05
-0.10
-0.15
-1
0
1
2
3
4
5
Gene Effect on SC GLS
B
Gene Effects on Growth
1.2
1.0
0.8
0.6
0.4
0.2
-0.2
-0.4
-1
0
1
2
3
4
5
Gene Effect on SC GLS
C
Gene Effects on Growth
1.2
1.0
0.8
0.6
0.4
0.2
-0.2
-0.4
-0.6
-0.15
-0.10
-0.05
0
0.05
-1
Gene Effect
on Flowering

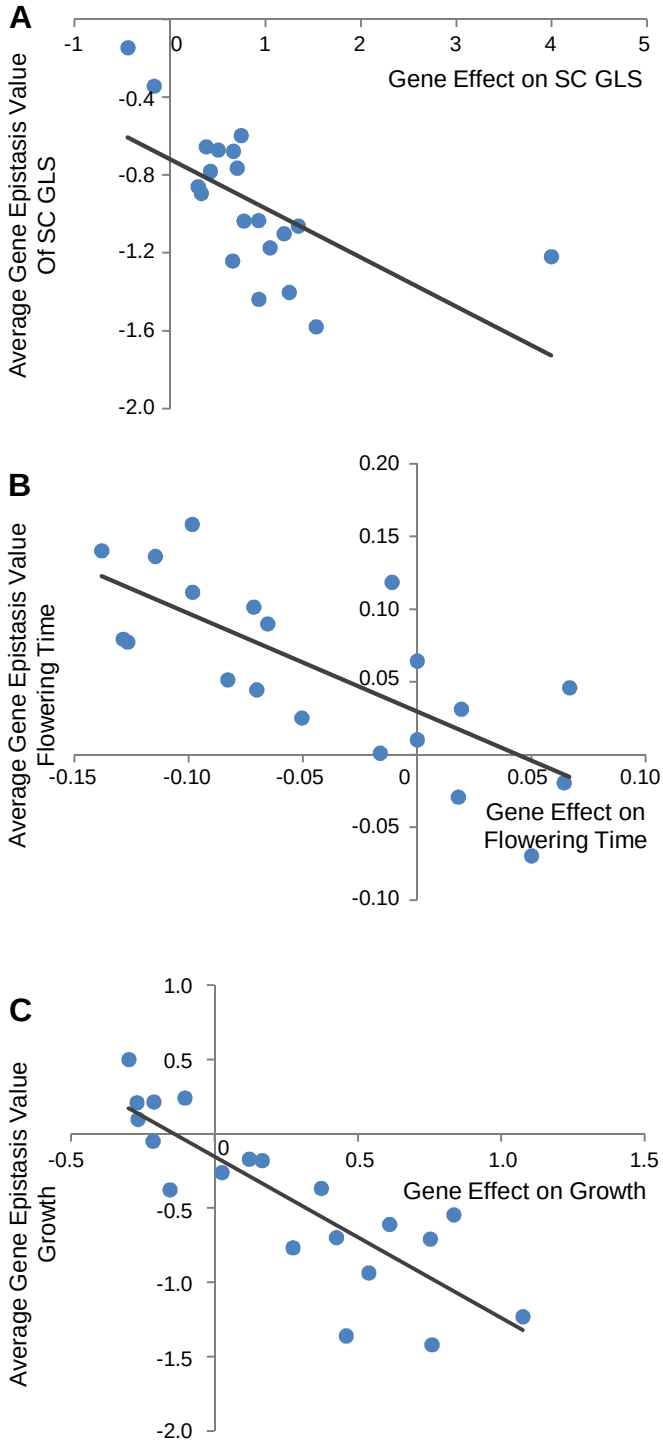
A
Average Gene Epistasis Value Of SC GLS
Gene Effect on SC GLS
-1
0
1
2
3
4
5
-0.4
-0.8
-1.2
-1.6
-2.0
B
Average Gene Epistasis Value Flowering Time
Gene Effect on Flowering Time
0.20
0.15
0.10
0.05
-0.05
-0.10
-0.15
-0.10
-0.05
0
0.05
0.10
C
Average Gene Epistasis Value Growth
Gene Effect on Growth
1.0
0.5
-0.5
-1.0
-1.5
-2.0
-0.5
0
0.5
1.0
1.5

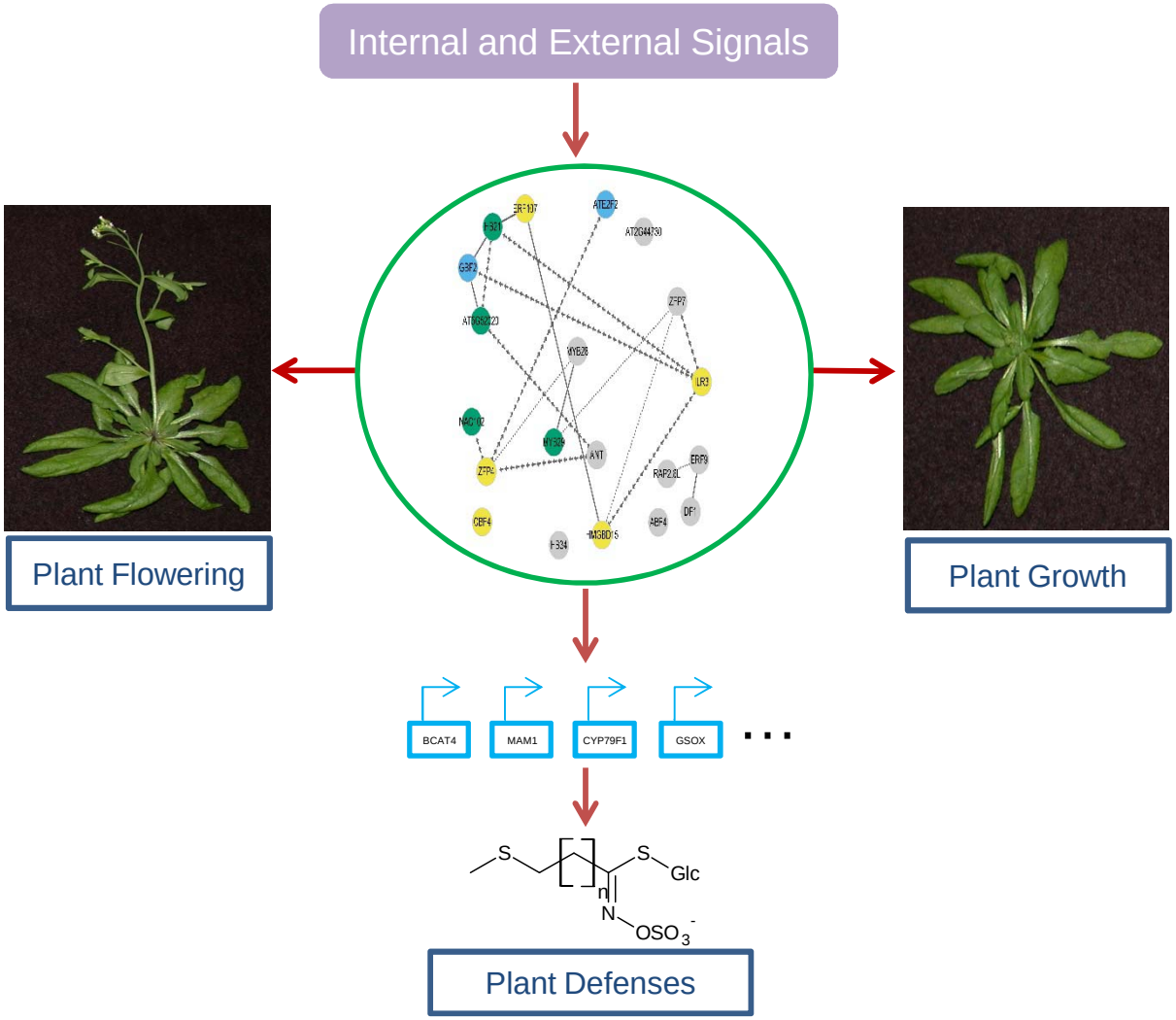
Internal and External Signals
Plant Flowering
Plant Growth
BCAT4
MAM1
CYP79F1
GSOX
Glc
Plant Defenses